Appendix

An algorithm is described for the determination of CL cross sections in the case that more than one reactant channel competes for a given CL channel. The attenuation of the metastable component $M^*(i)$ in the beam is governed by[12]

$$I_M{}^{*i} = I_M{}^{*i}(0) \exp(-n_{X_2} l \sigma_T) \quad \text{(A.1.a)}$$

$$= D_i(fA_{ki}) n_M{}^*(0) \exp(-n_{X_2} l \sigma_T) \quad \text{(A.1.b)}$$

where

$$D_i = S_\lambda{}^i(\Omega V/4\pi) \quad \text{(A.1.c)}$$

The detector factor D_i accounts for the solid angle Ω, the collision volume V viewed by the detector, and the detector efficiency $S_\lambda{}^i$ at the wavelength in question. f is the fraction of the emitter in the radiating fine structure state (e.g., $^3P_1$) and the other symbols have their usual meaning.[12] A_{ki} is the Einstein factor for spontaneous emission from M^*. For $Ca(^3P_1)$ this coincides with the measured lifetime,[55] but $Ca(^1D_2)$ is known[34,35] to decay radiatively by three competing pathways, and the relevant radiative lifetime is $\tau(^1D_2-{}^1S_1) = 25$ ms.[35]

In the cases (e.g., $Mg^* + X_2$[12]) where the observed CL derives from a single precursor, the CL intensity is[12-14]

$$I_{CL} = D_{CL} k_{CL} n_{X_2} n_M{}^* \quad \text{(A.2.a)}$$

$$= D_{CL} k_{CL} n_M{}^*(0) \exp(-n_{X_2} l \sigma_T)$$

where

$$D_{CL} = S_{\lambda'}{}^{CL}(\Omega V/4\pi) \quad \text{(A.2.b)}$$

The ratio of eqs A.1.b and A.2.a gives the well-known expression[12-14] for k_{CL} and σ_{CL}.

When more than one precursor competes for a product channel, eq A.2.a is modified to

$$I_{CL} = D_{CL} n_{X_2} n_M(0) \sum k_{CL}{}^j y_j \exp(-n_{X_2} l \sigma_T{}^j) \quad \text{(A.3)}$$

where $n_M(0)$ is the total unattenuated metal beam density, y_j is the fraction of the jth reactive beam component, and $\sigma_T{}^j$ is the corresponding attenuation cross section $\sigma_T(M^*(j))$ from Table I. As in the single-channel case, the ratio $I_{CL}/I_M{}^*(i)$ of CL and metastable emission intensities (here from $^3P_1$) defines, at the gas density $n_c{}^i$ where it is unity, the relation

$$I_{CL}/I_M{}^*(i) = C_i n_c{}^i [(\sum k_{CL}{}^j (y_j/y_i)) \exp(-n_c{}^i l(\sigma_T{}^j - \sigma_T{}^i))] \quad \text{(A.4.a)}$$

$$= 1$$

where

$$C_i = (S_{\lambda'}{}^{CL}/S_\lambda{}^i)(1/A_{ki} f_i) \quad \text{(A.4.b)}$$

For CaF_2 the three unknown $k_{CL}{}^j = \sigma_{CL}{}^j\langle v\rangle$, where ($j = {}^1S_0, {}^3P_1, {}^1D_2$), are obtained from eq A.4 by (1) setting $k_{CL}(^1D_2) = 0$, in accordance with the conclusions reached from Table I in section C.1, and (2) by switching the discharge off at $t = 0$, recording the CL intensity prior ($I_{CL}{}^-$) and immediately after ($I_{CL}{}^+$) the switch. The total metal beam flux was found almost unaffected by the discharge. The intensity ratio

$$(I_{CL}{}^-/I_{CL}{}^+) = [\sum k_{CL}{}^j \gamma_j \exp(-n_{X_2} l \sigma_T{}^j)]/k_{CL}{}^0 \exp(-n_{X_2} l \sigma_T{}^0) \quad \text{(A.5)}$$

$$= y_0 + (k_{CL}{}^1/k_{CL}{}^0) y_1 \exp(-n_{X_2} l(\sigma_T - \sigma_T{}^0))$$

provides one with the ratio $R = (k_{CL}{}^1/k_{CL}{}^0)$ of rate constants from ^3P and ^1S. Substituting R into (A.4) yields the desired expressions

$$k_{CL}{}^0 = [R + (y_0/y_1) \exp(-n_c{}^1 l(\sigma_T{}^1 - \sigma^0))]/C_i n_c{}^1 \quad \text{(A.6.a)}$$

$$k_{CL}{}^1 = R k_{CL}{}^0 \quad \text{(A.6.b)}$$

Registry No. Ca, 7440-70-2; Mg, 7439-95-4; F, 7782-41-4; Cl, 7782-50-5; Br, 7726-95-6.

(55) Furio, N.; Campbell, M. L.; Dagdigian, P. J. *J. Chem. Phys.* **1986**, *84*, 4332.

Photochemical Decomposition of Energetic Materials: Observation of Aryl Benzyloxy Nitroxide and Aryl Benzyl Nitroxide Radicals in Solutions of 1,3,5-Trinitrobenzene and Toluene and Their Deuteriated Analogues at 200 K

Joseph A. Menapace* and John E. Marlin

Frank J. Seiler Research Laboratory (AFSC), USAF Academy, Colorado 80840-6528
(Received: June 30, 1989)

Electron spin resonance spectroscopy is used to probe the photodecomposition of 1,3,5-trinitrobenzene (TNB) in toluene. The photodecomposition is conducted at 200 K with solutions containing TNB and toluene along with solutions containing their deuteriated analogues. Primary radicals observed in the decomposition have structures consistent with 3,5-dinitrophenyl benzyloxy nitroxide moieties. These radicals are proposed to be precursors to 3,5-dinitrophenyl benzyl nitroxide radicals previously observed in both photochemical and thermal decomposition. The aryl benzyloxy nitroxide radicals appear to decompose into 3,5-dinitrophenyl benzyl nitroxide radicals (secondary radicals) after the samples are allowed to remain at 200 K for extended time periods or after the solutions are warmed to 290 K. The secondary radicals observed in the study exhibit a temperature dependence involving the benzyl hydrogens adjacent to the nitroxide functionality. These hydrogens become magnetically inequivalent at low temperature, which may be attributed to the presence of different conformers of the aryl benzyl nitroxide species. Spectroscopic parameters for all the radicals observed are reported along with a proposed reaction scheme for the decomposition event.

I. Introduction

Electron spin resonance (ESR) spectroscopy has been widely used to identify paramagnetic reaction intermediates and to elucidate reaction kinetics and mechanisms in both the thermal and photochemical decomposition of explosives and propellants.[1-13] The impetus for these studies centers upon the notion that elu-

(1) Guidry, R. M.; Davis, L. P. *Thermochim. Acta* **1979**, *32*, 1.

cidation of the detailed nature of the decomposition event could lead to a means of modifying the material to minimize its sensitivity to environmental or chemical shock. Furthermore, understanding the details of the decomposition processes exhibited by these classes of compounds may lead to the synthesis of new energetic materials possessing improved chemical and mechanical properties that would ultimately yield explosives and propellants that are more energetic, yet more stable. These chemical and physical properties are of vital importance to both the civilian and military communities as energetic materials can be subjected to extreme conditions while in storage or in transit or while being prepared for use.

This paper reports our recent observation and identification of heretofore undetected reactive paramagnetic intermediates present in the early stages of the photochemical decomposition of 1,3,5-trinitrobenzene in toluene solution. The intermediates observed include the 3,5-dinitrophenyl benzyloxy nitroxide radical and its perdeuterio analogues that are produced by ultraviolet irradiation of the following solutions at 200 K: (1) 1,3,5-trinitrobenzene (TNB) in toluene; (2) perdeuterio-1,3,5-trinitrobenzene (TNB-d_3) in toluene; (3) 1,3,5-trinitrobenzene in perdeuteriotoluene (toluene-d_8); and (4) perdeuterio-1,3,5-trinitrobenzene in perdeuteriotoluene. Secondary radicals are also observed in the solutions, which are attributed to 3,5-dinitrophenyl benzyl nitroxide radicals similar to those characterized in previous studies.[1,2,4,14,20]

Thermal decomposition studies (ca. 470–520 K) on 2,4,6-trinitrotoluene[1,2,4] (TNT) using ESR spectroscopic techniques suggest that the earliest observed radical in the decomposition can be attributed to an aryl benzyl nitroxide moiety. This radical is presumably formed by the coupling of two TNT molecules in a "head-to-tail" configuration where a 2,4,6-trinitrobenzyl radical couples with a 2,6-dinitro-4-nitrosotoluene intermediate that is formed by reduction of the para nitro functionality on TNT. In these situations, the precursor to the nitrosobenzene intermediate is presumed to be an aryl benzyloxy nitroxide or aryl hydroxy nitroxide species; however, experimental ESR evidence for either of these particular radicals was not obtained. Existence of the 2,4,6-trinitrobenzyl radical has been suggested during TNT thermal decomposition in both isothermal differential scanning calorimetry[15] and solid TNT laser initiation experiments.[16] Participation by the aryl hydroxy nitroxide species has also been suggested in the thermal decomposition of TNT.[15] In this case, the decomposition rate was accelerated when hydrogen donor additives such as hydroquinone were present in the samples. Similar results have been obtained for the thermal decomposition of TNB when hexamethylbenzene is used as a benzyl radical source.[2]

Several photochemical decomposition studies utilizing ESR spectroscopy on TNT, TNB, and similar compounds show that aryl benzyl nitroxide,[14,17,20] aryl alkyl nitroxide,[3,14,20–22] diaryl nitroxide,[14] and aryl alkyloxy nitroxide[3,18–24] radicals are generated by ultraviolet photolysis of room-temperature solutions containing the nitroaromatic compounds and various solvents. The formation of the aryl alkyloxy nitroxide radicals in these studies is attributed to the solvolysis of the nitroaromatic compound with a solvent containing a labile hydrogen. The initiation of these reactions is reported to occur via hydrogen abstraction from the solvent by an excited triplet state of the nitroaromatic species. Once formed, the resulting solvent radical attacks the nitro functionality to produce the aryl alkyloxy nitroxide radical. In some cases, secondary radicals are observed that are attributed to aryl alkyl nitroxide moieties produced by the reactions analogous to those occurring in the thermal decomposition studies. Here, the dissociation of the aryl alkyloxy nitroxide radical yields an alkoxy radical and an arylnitroso compound that subsequently reacts with another solvent radical to produce the aryl alkyl nitroxide species.

The present study involves photolysis of solutions maintained at low temperature (200 K). In light of the previous studies conducted using thermal decomposition and room-temperature photochemical decomposition techniques, our strategy entails using the low-temperature environment to slow down the decomposition process to a point that may allow for the observation of paramagnetic species that are precursors to the aryl benzyl nitroxide radical. TNB was chosen for use in the experiments as it offers the opportunity to study the reactions via analysis of ESR spectra that are not complicated by the methyl hydrogen splittings present in radicals generated from TNT. Additionally, TNB maintains, as closely as possible, the major structural features possessed by TNT as well as eliminates the possibility of intramolecular reaction between the ortho nitro groups and the methyl group that may occur in TNT decomposition.[1–4,17] Toluene was chosen as the solvent in the reaction as it can be used as a source of benzyl radicals that are similar to those that may be present in the decomposition of neat TNT. The present experiments were designed to answer four questions important to the decomposition event: (1) Can precursors to the aryl benzyl nitroxide species be isolated in the low-temperature environment in sufficient quantity to be observed via ESR spectroscopy? (2) What are the relative stabilities of these radicals? (3) What are the identities of the paramagnetic precursors to the aryl benzyl nitroxide radical in the decomposition event? (4) What are the spectroscopic characteristics of these species?

II. Experimental Procedures

The TNB[25] and TNB-d_3[26] samples used in the study were prepared by personnel from the Frank J. Seiler Research Laboratory Energetic Materials Division using established synthetic procedures. The samples were purified by recrystallization in absolute ethanol and vacuum dried for 8 h at room temperature before use. HPLC-grade toluene (99.9%, Aldrich Chemical) and toluene-d_8 (99.5%, Stohler Isotope Chemicals) samples were used without further purification.

The ESR spectra were collected with a Varian Model E109 ESR spectrometer operating in the first-derivative mode. A TE_{102} rectangular cavity equipped with a horizontal grid to allow in situ ultraviolet irradiation of the solutions was used in all experiments. The ESR spectrometer magnetic field was controlled with a Varian Model E-272B field/frequency lock accessory equipped with an internal 1,1-diphenyl-2-picrylhydrazyl (DPPH) standard reference. The ESR spectrometer modulation frequency was set at 100 kHz, the modulation amplitude was set at 0.2 G peak to peak, and the incident microwave power was set at 20 mW. The isotropic g values for the radicals observed in the study were determined with

(2) McKinney, T. M.; Warren, L. F.; Goldberg, I. R.; Swanson, J. T. *J. Phys. Chem.* **1986**, *90*, 1008.
(3) Davis, L. P.; Wilkes, J. S.; Pugh, H. L.; Dorey, R. C. *J. Phys. Chem.* **1981**, *85*, 3505.
(4) Swanson, J. T.; Davis, L. P.; Dorey, R. C.; Carper, W. R. *Magn. Reson. Chem.* **1986**, *24*, 762.
(5) Britt, A. D.; Pace, M. D.; Moniz, W. B. *J. Energ. Mater.* **1983**, *1*, 367.
(6) Pace, M. D.; Britt, A. D.; Moniz, W. B. *J. Energ. Mater.* **1983**, *1*, 141.
(7) Pace, M. D.; Holmes, B. S. *J. Magn. Reson.* **1983**, *52*, 143.
(8) Pace, M. D.; Moniz, W. B. *J. Magn. Reson.* **1982**, *47*, 510.
(9) Pace, M. D. *Mol. Cryst. Liq. Cryst.* **1988**, *156*, 167.
(10) Glarum, S. H.; Marshall, J. H. *J. Chem. Phys.* **1964**, *41*, 2182.
(11) Freed, J. H.; Fraenkel, G. K. *J. Chem. Phys.* **1964**, *41*, 699.
(12) Noris, A. R.; Breck, A.; Depew, W.; Wan, J. K. S. *Can. J. Chem.* **1970**, *48*, 3440.
(13) Gupta, R. K.; Subramanian, J.; Ray, N. K.; Narisimham, P. T. *Chem. Phys. Lett.* **1968**, *2*, 150.
(14) Ayscough, P. B.; Sealy, R. C.; Woods, D. E. *J. Phys. Chem.* **1971**, *75*, 3454.
(15) Shackelford, S. A.; Beckmann, J. W.; Wilkes, J. S. *J. Org. Chem.* **1977**, *42*, 4201.
(16) Capellos, C.; Iyer, S. 10th ICT Conference: Combustion and Detonation Phenomena, Karlsruhe, FRG, 27–29 Jun 1979; Paper 33. Papagiannacopoulos, P.; Capellos, C. NATO Advanced Study Institute on Chemical Reaction Dynamics, Iraklion (Crete), GR, 27 Aug–7 Sep 1985.
(17) Burlinson, N. E.; Sitzman, M. E.; Kaplan, L. A.; Kayser, E. *J. Org. Chem.* **1979**, *44*, 3695.
(18) Janzen, E. G.; Gerlock, J. L. *J. Am. Chem. Soc.* **1969**, *91*, 3108.
(19) Cowley, D. J.; Sutcliffe, L. H. *Chem. Commun.* **1968**, 201.
(20) Wong, S. K.; Wan, J. K. S. *Can. J. Chem.* **1973**, *51*, 753.
(21) Sleight, R. B.; Sutcliffe, L. H. *Trans. Faraday Soc.* **1971**, 2195.
(22) Cowley, D. J.; Sutcliffe, L. H. *J. Chem. Soc. B* **1970**, 569.
(23) Paton, R. M.; Weber, R. U. *Org. Magn. Reson.* **1977**, *8*(9), 494.
(24) Ward, R. L. *J. Chem. Phys.* **1963**, *38*, 2588.
(25) Clarke, H. T.; Hartman, W. W. *Organic Synthesis*; Wiley: New York, 1932; Collect. Vol. 1, p 541.
(26) Buncel, E.; Symons, E. A. *Can. J. Chem.* **1966**, *44*, 771.

the field/frequency lock calibrated by an Eldorado Instruments Model 990G microwave frequency counter and a solid DPPH sample. The calibration was such that the center of the spectrum for the solid DPPH sample was at the center of the magnetic field sweep. Sample isotropic g values were calculated assuming a g value of 2.0036 ± 0.0003 for DPPH.[27]

Sample temperature was established and maintained with a Bruker Model ER-4111 VT temperature control accessory using a combination of liquid nitrogen, heating Dewar interconnections, and transfer Dewars to direct nitrogen gas of a particular temperature over the sample in the ESR cavity. The sample temperature was monitored with a Luxtron Model 750 fluoroptic thermometry system equipped with a MIW-type fluoroptic temperature probe. The temperature probe tip was placed into a quartz capillary tube that was sealed on one end. The entire probe assembly was then inserted into the ESR tube containing the liquid sample, which allowed for in situ sample temperature measurement.

The solutions were irradiated in the ESR cavity with an Oriel 1000-W Hg/Xe (Hanovia Model L5173) high-pressure arc source located 40 cm from the ESR cavity irradiation grid. The light was collimated into the cavity grid with use of extreme care not to focus the light beam in the sample cavity. This enabled the sample to be adequately irradiated while avoiding sample heating during the experiments. A lower wavelength limit was established at 190 nm for the incident ultraviolet light used in the experiments by placing a water bath between the arc source and the ESR sample cavity.

The photochemical decomposition was accomplished by placing 0.35 mL of solution, 0.01 M TNB or TNB-d_3, respectively (toluene or toluene-d_8 used as solvent), into a Suprasil quartz ESR sample tube (Wilmad Model 707-SQ). The sample was then placed into the sample cavity of the ESR spectrometer that was maintained at 200.0 ± 0.5 K. After the sample temperature equilibrated to 200 K (usually 30-min equilibration time), the solution was irradiated with the Hg/Xe arc source. Care was taken not to heat the sample during irradiation by using minimum arc source lamp power. Irradiation was continued for approximately 15 min after which ESR spectra of the primary radicals were collected and stored on a microcomputer using software developed in this laboratory for ESR data collection and analysis.[28] In some experiments, samples were kept at 200 K in the ESR spectrometer for extended time periods, in some cases up to 6 h. ESR spectra were then taken of secondary radicals formed during this dark period. In other experiments, the sample temperature was increased to 290 K after ESR spectra of the primary radicals were collected. At this point, room-temperature ESR spectra of the secondary radicals were obtained. The sample temperature was once again lowered to 200 K, and ESR spectra of the secondary radicals were collected at low temperature. In all cases, the same secondary radicals were observed regardless of whether the samples were allowed to remain in the cold environment for extended time periods or whether they were heated to room temperature (290 K) and then subsequently cooled to 200 K. The ESR spectra were subsequently analyzed via computer, and spectral simulations were conducted for the radicals observed. The parameters used in the simulations were determined from the experimental ESR spectra and included the hyperfine splittings for the various spin species present and the average first-derivative peak-to-peak line width. The applied simulation algorithms assume that the ESR spectra are composed of features possessing Lorentzian line shapes. The ESR spectra were also corrected for base-line offset and base-line drift with an ESR spectrum base-line correction computer program developed at this laboratory.[29]

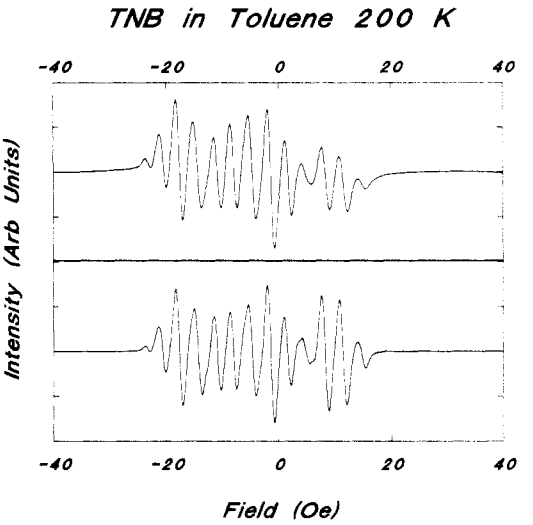

Figure 1. ESR spectrum collected after 15 min of ultraviolet irradiation of a TNB/toluene sample at 200 K. The upper trace corresponds to the experimental ESR spectrum. The lower trace corresponds to the spectrum simulation. Spectral parameters are presented in Table I and in the text.

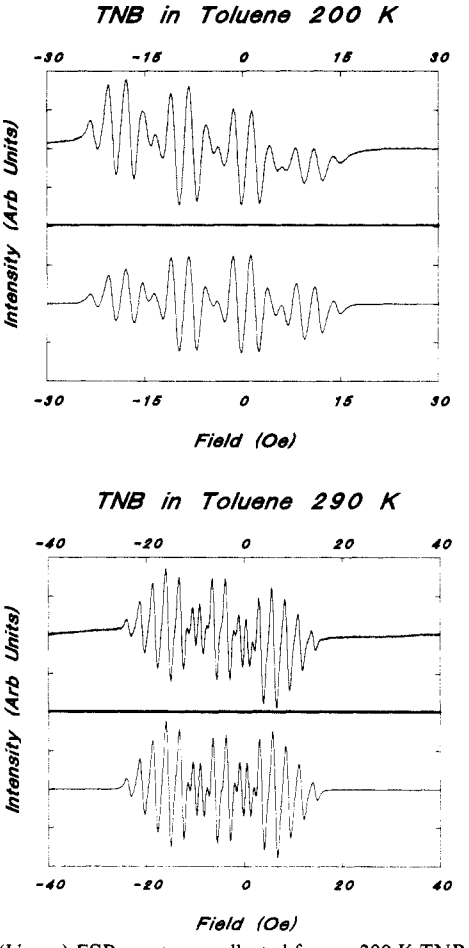

Figure 2. (Upper) ESR spectrum collected from a 200 K TNB/toluene solution during a dark reaction proceeding 4 h after sample irradiation was terminated. (Lower) ESR spectrum collected from a 290 K TNB/toluene solution after photolysis. The top traces of each set correspond to the experimental ESR spectra. The bottom traces of each set correspond to the spectral simulations. Spectral parameters are presented in Table I and in the text.

III. Results

A. Photochemical Decomposition of TNB in Toluene. Figures 1 and 2 present the experimental results and the corresponding spectral simulations for the radicals observed in the photochemical decomposition of TNB in toluene. The ESR spectrum shown in

(27) Alger, R. S. *Electron Paramagnetic Resonance: Techniques and Applications*; Wiley: New York, 1968; p 414.
(28) Anderson, D. R.; O'Neill, M. V.; Swanson, J. T. Unpublished software.
(29) Menapace, J. A. Technical Report FJSRL-TR-89-0003, ADA No. 207065; Frank J. Seiler Research Laboratory, USAF Academy; Colorado Springs, CO, Mar 1989.
(30) McMillan, M.; Norman, R. O. C. *J. Chem. Soc. B* **1968**, 590.

TABLE I: Spectroscopic Characteristics for Radicals Observed during Photodecomposition of TNB in Toluene

radical species[a]	temp, ±0.5 K	a_N, Oe	a_N,[d] Oe	a_H,[c] Oe	a_{CH_2}, Oe		lw[b]	g value (±0.0003)
I(a)	200	12.90	0.25	3.27	0.45	0.45	0.65	2.0051
II(a)	200	9.52	0.20	2.68	4.96	4.96	0.75	2.0061
II(b)		9.52	0.20	2.68	6.71	3.21	0.75	
II(c)	290	9.52	0.20	2.68	5.36	5.36	0.75	2.0061
III(a)	200	12.90	0.25	3.27	0.05	0.05	0.95	2.0051
IV(a)	200	9.52	0.20	2.68	0.72	0.72	0.95	2.0061
IV(b)		9.52	0.20	2.68	0.97	0.47	0.95	
IV(c)	290	9.52	0.20	2.68	0.73	0.73	0.85	2.0061
V(a)	200	12.90	0.25	0.50	0.45	0.45	1.10	2.0051
VI(a)	200	9.52	0.20	0.41	4.96	4.96	1.10	2.0061
VI(b)		9.52	0.20	0.41	6.71	3.21	1.10	
VI(c)	290	9.52	0.20	0.37	5.36	5.36	0.75	2.0061
VII(a)	200	12.90	0.25	0.50	0.05	0.05	1.10	2.0051
VIII(a)	200	9.52	0.20	0.41	0.72	0.72	1.10	2.0061
VIII(b)		9.52	0.20	0.41	0.97	0.47	1.10	
VIII(c)	290	9.52	0.20	0.37	0.73	0.73	1.10	2.0061
IX	290	15.18	1.02[e]	3.03	0.35[f]		0.30	2.0052
X	290	13.30	0.25	3.00	0.45[f]		0.65	2.0051
XI	290	11.84	0.99[e]	3.03	5.84[f]		0.65	2.0061
XII	290	9.69	0.25	2.55	4.70[f]		1.00	2.0061

[a] The radicals corresponding to the numbered entries are referenced in the text. [b] Line widths are measured as peak-to-peak values from the first-derivative ESR spectra. [c] Ortho and para hydrogens in 1,3,5-trinitrophenyl subunit. [d] Meta nitro group nitrogens in 1,3,5-trinitrophenyl subunit. [e] Meta hydrogens in phenyl subunit. [f] Hydrogen on THF subunit.

Figure 1 is obtained after 15 min of irradiation of a TNB/toluene sample maintained at 200 K. Measurement of the hyperfine splittings and the ESR peak intensities shows that the spectrum is composed of an admixture of three radical species that can be associated with the 3,5-dinitrophenyl benzyloxy nitroxide (I) and

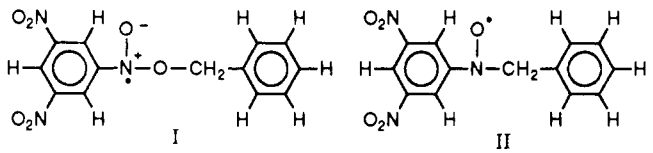

I II

two conformational isomers of 3,5-dinitrophenyl benzyl nitroxide (II) radicals (vide infra). Spectral simulation yields a spectrum (Figure 1 and Table I) that is consistent with the experimental spectrum being composed of 53.2% species I(a), 26.6% species II(a), and 20.2% species II(b). The g values for radicals I and II are 2.0051 ± 0.0003 and 2.0061 ± 0.0003, respectively. The upper trace in Figure 2 shows the ESR spectrum of radicals that are produced during the dark reaction at 200 K. After 4 h at 200 K, the TNB/toluene sample contains paramagnetic species that can be assigned to radical II. The upper spectrum in Figure 2 is composed of two conformational isomers of II (42.9% species II(a) and 57.1% species II(b)) with hyperfine splitting constants and line widths as shown in Table I. In this case, the g value for the radicals is 2.0061 ± 0.0003. The lower trace in Figure 2 shows an ESR spectrum of the TNB/toluene sample after the sample has been heated to 290 K. The spectra consists of 100% species II(c). Subsequently cooling the sample yields a spectrum identical with that shown in the upper trace of Figure 2.

B. Photochemical Decomposition of TNB in Toluene-d_8. Photochemical decomposition of TNB/toluene-d_8 solutions yields the ESR spectra presented in Figures 3 and 4. The spectrum shown in Figure 3 is observed after the solution of TNB/toluene-d_8 maintained at 200 K is irradiated for 15 min. Analysis of the spectrum indicates that three paramagnetic species contribute to the observed signal whose structures are consistent with 3,5-dinitrophenyl benzyloxy-d_7 nitroxide (III) and 3,5-dinitrophenyl

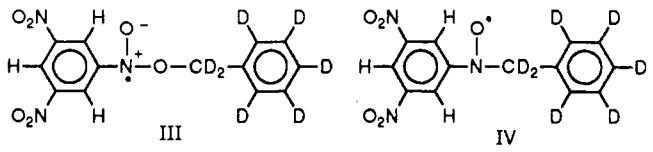

III IV

benzyl-d_7 nitroxide (IV) radicals (two conformational isomers). The computer-simulated spectrum in Figure 3 is consistent with

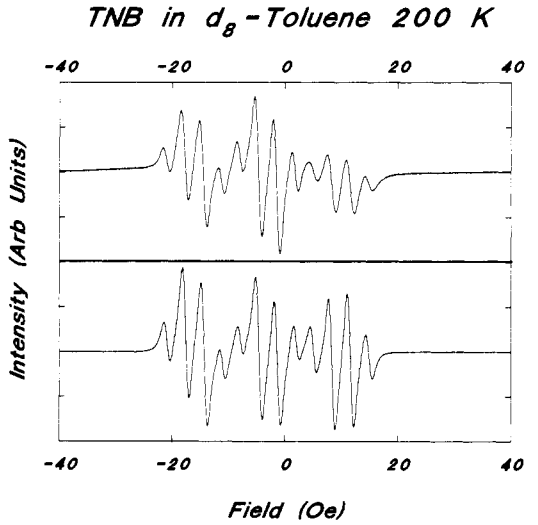

Figure 3. ESR spectrum collected after a 15-min ultraviolet irradiation of a TNB/toluene-d_8 sample at 200 K. The upper trace corresponds to the experimental ESR spectrum. The lower trace corresponds to the spectral simulation. Spectral parameters are presented in Table I and in the text.

the experimental spectrum with the results of this analysis showing that the spectrum can be attributed to 53.2% species III(a), 26.6% species IV(a), and 20.2% species IV(b) with the spectroscopic properties as shown in Table I. The g values for radicals III and IV in this spectrum are 2.0051 ± 0.0003 and 2.0061 ± 0.0003, respectively. After 6 h at 200 K, the TNB/toluene-d_8 sample yields an ESR spectrum shown in the upper trace of Figure 4. This spectrum corresponds to radical IV, which is produced during the dark reaction. The simulated spectrum establishes that this spectrum can be attributed to 41.2% species IV(a) and 58.8% species IV(b). The lower trace on Figure 4 presents the ESR spectrum of the radical present in a TNB/toluene-d_8 sample that was irradiated at 200 K and was subsequently heated to 290 K. This spectrum corresponds to radical IV (100% species IV(c)) with the spectroscopic properties shown in Table I. Again, subsequent cooling of the sample yields a spectrum identical with that shown in the upper trace of Figure 4.

C. Photochemical Decomposition of TNB-d_3 in Toluene. The ESR spectra collected during the photochemical decomposition of TNB-d_3/toluene solutions are shown in Figures 5 and 6 along with their corresponding simulated spectra. The spectrum shown

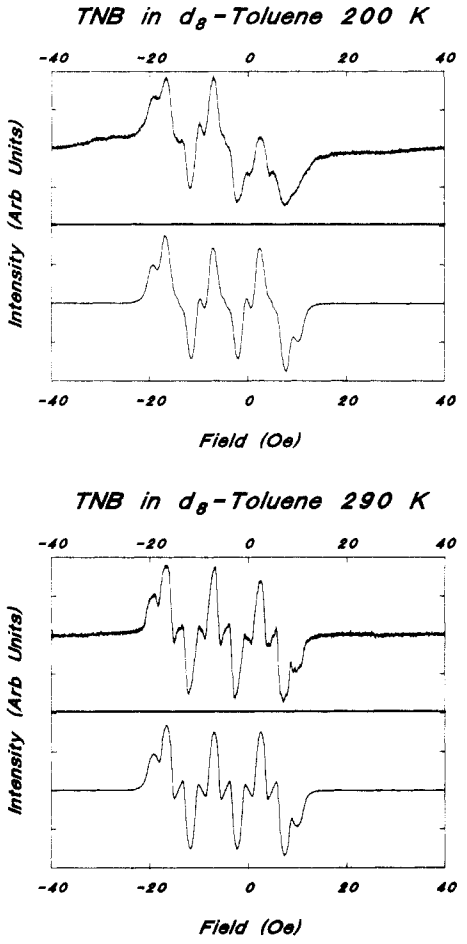

Figure 4. (Upper) ESR spectrum collected from a 200 K TNB/toluene-d_8 solution during a dark reaction that was continued for 6 h after sample irradiation. (Lower) ESR spectrum collected from a 290 K TNB/toluene-d_8 solution after photolysis. The top traces of each set correspond to the experimental ESR spectra. The bottom traces of each set correspond to the spectral simulations. Spectral parameters are given in Table I and in the text.

in Figure 5 corresponds to the first radical ESR spectrum observed subsequent to ultraviolet irradiation of the sample at 200 K. Measurement of the hyperfine splittings and ESR peak intensities (Table I) suggests that this spectrum contains 3,5-dinitrophenyl-d_3 benzyloxy nitroxide (V) and two conformational isomers of 3,5-

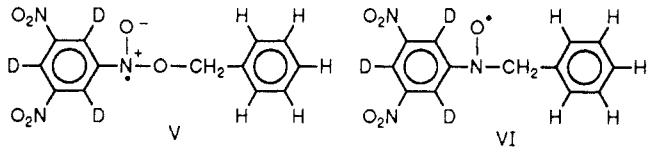

dinitrophenyl-d_3 benzyl nitroxide (VI) radicals. The results of the spectral simulation indicate that the spectrum observed is composed of 37.6% species V(a), 24.8% species VI(a), and 37.6% species VI(b) (see Table I). The spectrum shown in the upper trace of Figure 6 corresponds to radicals produced during the dark reaction 6 h after the photodecomposition is initiated. The spectrum is best attributed to radical VI with an admixture of 60.6% species VI(a) and 39.4% species VI(b) (see Table I). The lower trace in Figure 6 presents the spectrum observed after the TNB-d_3/toluene sample was allowed to react at 200 K and then subsequently heated to 290 K. This spectrum is attributed to a single species VI(c) possessing the spectroscopic properties listed in Table I. Temperature cycling between 200 and 290 K provided spectra identical with those shown in the upper and lower traces of Figure 6, respectively.

D. Photodecomposition of TNB-d_3 in Toluene-d_8. The ESR spectra and computer simulations pertaining to the photochemical decomposition of TNB-d_3/toluene-d_8 solutions are presented in

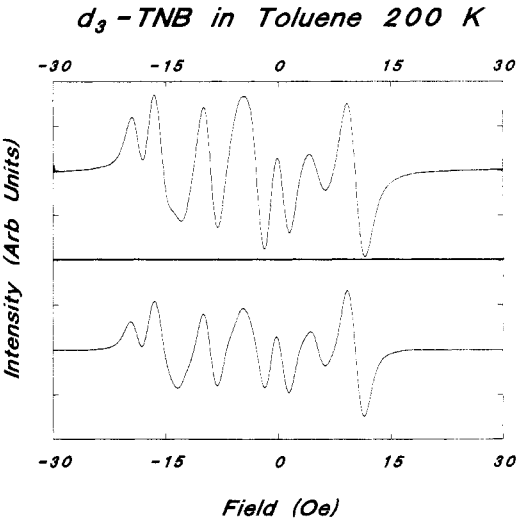

Figure 5. ESR spectrum collected after photolyzing a TNB-d_3/toluene sample at 200 K for 15 min. The upper trace corresponds to the experimental ESR spectrum. The lower trace corresponds to the spectral simulation. Spectral parameters are in Table I and in the text.

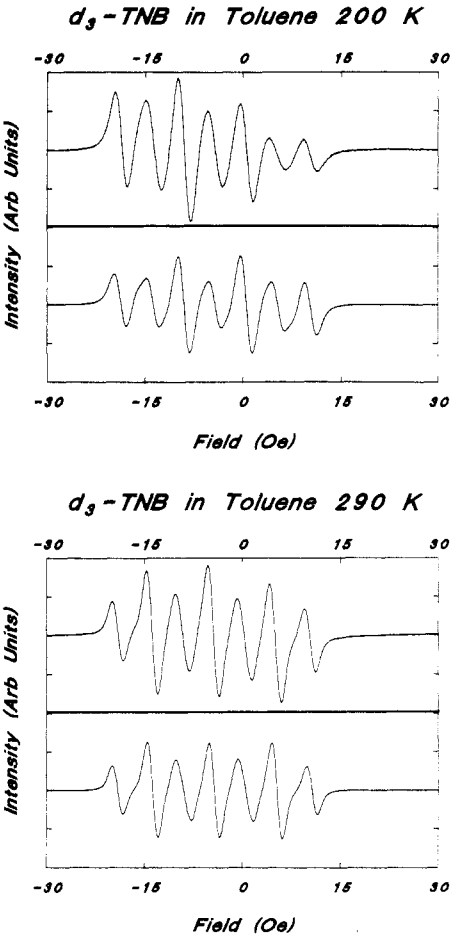

Figure 6. (Upper) ESR spectrum collected from a 200 K TNB-d_3/toluene solution during a dark reaction proceeding 6 h after sample irradiation. (Lower) ESR spectrum collected from a 290 K TNB-d_3/toluene solution after photolysis. The top traces of each set correspond to the experimental ESR spectra. The bottom traces of each set correspond to the spectral simulations. Spectral parameters are presented in Table I and in the text.

Figures 7 and 8. The spectrum shown in Figure 7 corresponds to the primary radicals observed after a 15-min ultraviolet irradiation of the sample maintained at 200 K. Measurement of the hyperfine splittings and ESR signal intensities and subsequent spectral simulation suggest that this spectrum contains 48.5% species VII(a), 30.3% species VIII(a), and 21.2% species VIII(b)

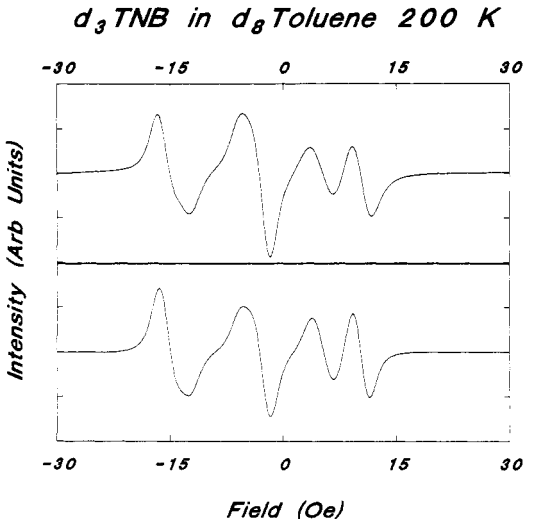

Figure 7. ESR spectrum collected after a 15-min ultraviolet irradiation of a TNB-d_3/toluene-d_8 sample at 200 K. The upper trace corresponds to the experimental ESR spectrum. The lower trace corresponds to the spectrum simulation. Spectral parameters are given in Table I and in the text.

(two conformational isomers) possessing the spectral properties outlined in Table I. These radicals are consistent with species whose structures are attributed to 3,5-dinitrophenyl-d_3 benzyloxy-d_7 nitroxide (VII) and 3,5-dinitrophenyl-d_3 benzyl-d_7 nitroxide

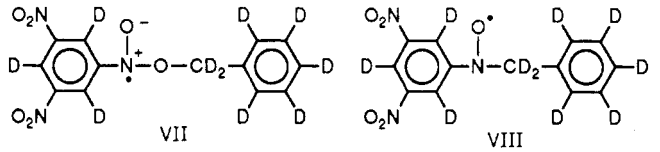

(VIII) radicals. The upper trace of Figure 8 presents the ESR spectrum containing secondary radicals formed during the dark reaction that continued for 5 h after initial irradiation of the sample. This spectrum consists of 41.2% species VIII(a) and 58.8% species VIII(b) as determined from spectral simulation. Radical VIII is also observed (100% species VIII(c)) after the sample is heated to 290 K (lower trace of Figure 8). Subsequent cooling of the TNB-d_3/toluene-d_8 sample to 200 K yields a spectrum identical with that shown in the upper trace of Figure 8 consisting of the secondary radicals.

IV. Discussion

A. 3,5-Dinitrophenyl Benzyloxy Nitroxide Radicals. The ESR spectra collected during the initial stages of photodecomposition exhibit hyperfine splittings, signal intensity ratios, and g values consistent with radicals whose molecular structures support assignment as aryl benzyloxy nitroxide moieties. The primary radicals resulting from reaction between TNB (TNB-d_3) and toluene (toluene-d_8) yield ESR spectra (Figures 1, 3, 5, and 7) composed primarily of signal splittings that can be attributed to hyperfine splittings from the nitroxide nitrogen and the three aryl hydrogens (ortho and para to the nitroxide functionality). The hyperfine splittings from the aryl nitro group nitrogens and the benzyloxy hydrogens in these radicals are small and cannot be unambiguously identified. The assignment of hyperfine splittings from these atoms are considered only tentative as they are determined by careful examination of ESR peak shoulders and signal line shape. Computational modeling of the spectra suggests that a first-derivative peak-to-peak line width of 0.20 Oe (assuming a Lorentzian line shape) is necessary to properly resolve the small splittings from the meta substituents and the benzyloxy hydrogens. The line widths observed in this study range from 0.65 to 1.10 Oe. The ESR spectra suggest that the aryl benzyloxy nitroxide radicals are generated in the low-temperature environment along with secondary radicals that can be assigned to aryl benzyl nitroxide moieties. This is not surprising as one would not expect to observe ESR spectra that are free of secondary radical contamination since experimental observation indicates that the primary radicals are relatively unstable when compared with the secondary radicals. Photodecomposition conducted at room temperature yields only aryl benzyl nitroxide radicals. Furthermore, after extended time periods at 200 K or after the solutions are heated to 290 K, the aryl benzyloxy nitroxide radicals apparently decompose to the more stable aryl benzyl nitroxide species. These experimental observations suggest that significant amounts of secondary radicals are produced very early in the decomposition and that the primary radical precursors are most likely observed because their decomposition rates are slow enough at the low temperatures to yield detectable radical concentrations. A semiquantitative assessment of the relative amounts of the aryl benzyloxy nitroxide and aryl benzyl nitroxide radicals present is obtained from the computer simulations of the ESR spectra. The composition of each paramagnetic species contributing to the spectra is presented in the Results as percent composition. The simulations suggest that spectra collected 15 min after the initiation of photodecomposition contain approximately equimolecular concentrations of both species.

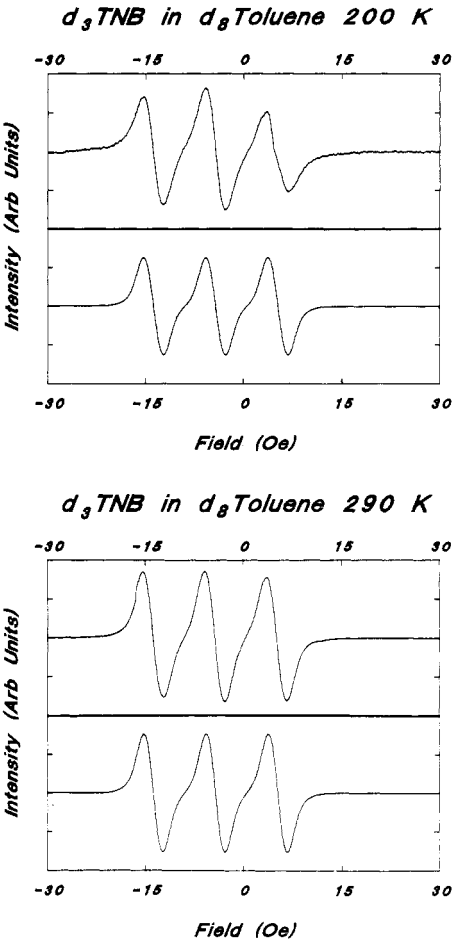

Figure 8. (Upper) ESR spectrum collected from a 200 K TNB-d_3/toluene-d_8 solution during a dark reaction proceeding 5 h after sample irradiation. (Lower) ESR spectrum collected from a 290 K TNB-d_3/toluene-d_8 solution after photolysis. The top traces of each set correspond to the experimental ESR spectra. The bottom traces of each set correspond to the spectral simulations. Spectral parameters are presented in Table I and in the text.

The primary and secondary radicals present in the initial stages of the TNB/toluene photodecomposition (Figure 1) are assigned with the assumption that the spectrum for radical I is approximately four times more intense than the spectrum corresponding to radical II if one assumes that equal numbers of radicals of the two types are present. The difference in signal intensity can be attributed to large additional splittings (ca. 3–7 Oe) present in radical II that arise from the benzyl hydrogens. These hydrogens cause almost four times as much signal splitting than that present in radical I. Comparison of the spectra in Figures 1 and 2 (upper

trace) shows that the species present in the former spectrum possess a low-field wing intensity ratio of 1.0:5.8:13.2:9.4:7.7, while those present in the latter spectrum possess a ratio of 1.0:3.1:3.4:1.2. If one considers that the spectrum in Figure 1 contains aryl hydrogen quartets in the low-field wing for both radical I and radical II, the intensity ratio should be 1.0:5.9:13.9:9.9:8.1 based upon spectral simulation (Figure 1) that includes the relative amounts of the species present as well as the differences in their corresponding g values.

The ESR spectrum providing unambiguous evidence for the presence of the aryl benzyloxy nitroxide radical involves the photodecomposition of TNB in toluene-d_8 (Figure 3). Deuteriation of toluene in this study simplifies the spectrum of the aryl benzyl nitroxide radical that contributes to the ESR spectrum. The spectrum is assigned with the assumption that the signal intensity from radical III is approximately equal to the signal intensity from radical IV if the species are present in equal concentration. As with the TNB/toluene spectrum, this is due to the splittings from the benzyl protons in the aryl benzyl nitroxide radical. The primary and secondary radicals present immediately after irradiating the sample yield a spectrum consisting of quartets due to the aryl hydrogen splittings ($a_H(3)$ = 3.27 Oe) in a 1:3:3:1 intensity ratio that is further split into a triplet (1:1:1) by nitrogen with a hyperfine splitting of a_N = 12.90 Oe. With deuteriation, radical IV should possess benzyl hydrogen hyperfine splittings approximately 1/6.5 ($\mu_D I_H/\mu_H I_D$ for which $\mu_N = g_N\beta_N I_N$) that of the corresponding protonated radical;[31] that is, radical IV should possess benzyl hydrogen hyperfine splittings of a_H = 1.03, 0.49 Oe and $a_H(2)$ = 0.76 Oe for each contributing conformational isomer of aryl benzyl nitroxide species. On the basis of spectral analysis and computational modeling of the spectrum, the benzyl hydrogen hyperfine splittings for the two species present are determined to be a_H = 0.97, 0.47 Oe and $a_H(2)$ = 0.72 Oe, respectively (upper trace of Figure 4 and Table I). Deuteriation of the benzyl subunit in these radicals confirms the assignment of the benzyl position hyperfine splittings and the presence of the different radical species. The net result of the presence of radical IV in the spectrum collected immediately after irradiation (Figure 3) is the appearance of a negative base-line slope through the quartet splittings seen in the radical III spectrum.

The ESR spectrum collected immediately after low-temperature irradiation of TNB-d_3 in toluene provides further evidence of the presence of the aryl benzyloxy nitroxide radical in the photodecomposition (Figure 5). This spectrum is mainly composed of a triplet (1:1:1) due to nitrogen hyperfine splitting (a_N = 12.90 Oe) from radical V superimposed on the spectrum of radical VI (upper trace of Figure 6). The spectrum of this latter species is composed of hyperfine splittings that are attributed to the benzyl hydrogens measured at a_H = 6.71, 3.21 Oe and $a_H(2)$ = 4.96 Oe for each conformational isomer of VI present. Deuteriation of TNB in these experiments yields the expected simplification of both the aryl benzyloxy nitroxide and aryl benzyl nitroxide radical contributions to the spectrum. In this case, the aryl hydrogen hyperfine splittings for the former radical are reduced to a_H = 0.50 Oe while the splittings in the latter radical are reduced to a_H = 0.41 Oe. Both of these values are in agreement with what one would expect from deuteriation based upon the theoretical arguments given for the TNB/toluene-d_8 case. Deuteriation of the TNB subunit in these radicals further confirms the assignment of the aryl hyperfine splittings. The spectrum is assigned with the assumption, as in the TNB/toluene case, that the aryl benzyloxy nitroxide radical signal intensity should be about four times greater than that of the corresponding aryl benzyl nitroxide radical.

Deuteriation of both TNB and toluene provides the simplest spectrum that identifies and characterizes the radicals present in the initial phases of the decomposition. The ESR spectrum shown in Figure 7 can be attributed to two sets of nitrogen triplets (1:1:1) arising from the aryl benzyloxy nitroxide and aryl benzyl nitroxide species. One set of triplets corresponding to a nitrogen hyperfine splitting of a_N = 12.90 Oe can be attributed to radical VII while the other triplet with a hyperfine splitting of a_N = 9.52 Oe can be attributed to radical VIII. The spectrum is assigned with use of an equal signal intensity assumption for the species present since only the nitrogen atoms provide significant spectral hyperfine splitting. Deuteriation of the reactants provides further evidence for the assignment of the aryl and benzyl hydrogen hyperfine splittings through comparison with the ESR spectra collected for the isotopic analogues.

The g value of 2.0051 ± 0.0003 determined from the aryl benzyloxy nitroxide radical spectra in Figures 1, 3, 5, and 7 is typical of the g values for this class of compounds.[23,30] To support the assignment, we reproduced the aryl alkyloxy nitroxide radical experiments previously reported for nitrobenzene and TNB in tetrahydrofuran (THF).[18-20,24] The radicals were prepared by photochemical decomposition at 290 K with the same procedures as described for the photochemical decomposition of TNB in toluene. Immediately after irradiation, primary radicals that can be attributed to aryl alkyloxy nitroxide radicals, IX and X, are

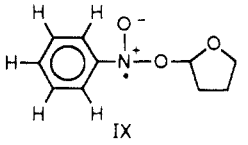

IX

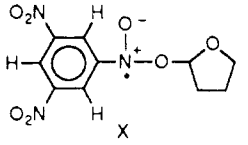

X

observed. The hyperfine splitting constants obtained are similar to those previously reported. For radical IX, the hyperfine splitting constants are measured at a_N = 15.18, $a_H(2)$ = 1.02, a_H = 0.35, and $a_H(3)$ = 3.03 Oe (Table I). For radical X, the hyperfine splitting constants are a_N = 13.30, $a_N(2)$ = 0.25, a_H = 0.45, and $a_H(3)$ = 3.00 Oe. The g values for the nitrobenzene/THF and TNB/THF primary radical adducts are 2.0052 ± 0.0003 and 2.0051 ± 0.0003, respectively.

Secondary radicals in the nitrobenzene/THF and TNB/THF photochemical decomposition are observed after the solutions are allowed to react during a dark period. The secondary radicals possess ESR spectra with characteristics consistent with assignment as aryl alkyl nitroxide species XI and XII. The hyperfine

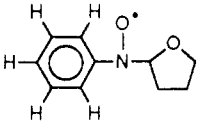

XI

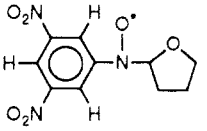

XII

splittings measured for radical XI are a_N = 11.84, $a_H(3)$ = 3.03, $a_H(2)$ = 0.99, and a_H = 5.84 Oe. The hyperfine splittings measured for radical XII are a_N = 9.69, $a_N(2)$ = 0.25, $a_H(3)$ = 2.55, and a_H = 4.70 Oe (Table I). The hyperfine splitting due to the hydrogen atom on THF β to the nitroxide functionality is characteristic of this class of compounds as indicated by the magnitude of the hyperfine splitting. Furthermore, the nitrogen and aryl hydrogen hyperfine splittings compare well with those observed for the specific radical class. The g values for radicals XI and XII are 2.0061 ± 0.0003 and 2.0061 ± 0.0003, respectively, in agreement with published values for radicals of this type.[33-35]

The hyperfine splittings measured from the aryl benzyloxy nitroxide radical spectra collected during the TNB (TNB-d_3)/toluene (toluene-d_8) photodecompositions are in good agreement with the known magnitudes measured in photodecomposition studies of TNB in THF[20,24] and other nitroaromatic compounds in various solvents.[18-24,30] The nitrogen hyperfine splitting of a_N = 12.90 Oe in the aryl benzyloxy nitroxide radicals from this study is in the range of a_N = 12–16 Oe characteristic of aryl alkyloxy nitroxide species. For the corresponding radical observed when nitrobenzene and THF undergo photochemical reaction, a nitrogen hyperfine splitting of a_N = 15.00 Oe[20,24] (a_N = 15.18 Oe vide

(31) *Handbook of Chemistry and Physics*, 59th ed.; CRC Press: West Palm Beach, FL, 1978; p E69.
(32) Baltrop, J. A.; Bunce, N. J. *J. Chem. Soc. C* **1968**, 1467.
(33) Wajer, T. A. J. W.; Mackor, A.; De Boer, T. J. *Tetrahedron* **1969**, *25*, 175.
(34) Joshi, A.; Yang, G. C. *Org. Magn. Reson.* **1981**, *17*, 138.
(35) Flesia, E.; Surzur, J.; Tordo, P. *Org. Magn. Reson.* **1978**, *11*, 123.

supra) is observed. Aryl alkyloxy nitroxide radicals[22] observed when 3-chloronitrobenzene and 3,5-dichloronitrobenzene are photolyzed in THF possess nitrogen hyperfine splittings of a_N = 14.15 and 14.00 Oe, respectively. The reduction in the nitrogen hyperfine splitting in these species may be due to σ-bond inductive effects caused by the presence of meta electron withdrawing groups on the aromatic ring. Similar results are obtained when 3-carboxy- and 3,5-dicarboxynitrobenzene compounds are photolyzed in THF.[21] On the basis of this notion, the nitrogen hyperfine splitting in the aryl benzyloxy nitroxide radicals under present study would be expected to be slightly lower since the nitro functionality is more effective at withdrawing electron density than both the Cl and COOH functionalities. The 12.90-Oe nitrogen hyperfine splitting observed in our studies is nearly the same as that recorded for TNB in THF (a_N = 13.00 Oe[20,24] and 13.30 Oe vide supra), which suggests that the same environment is present in the vicinity of the nitrogen in both radicals. The ortho and para hydrogen hyperfine splittings of $a_H(3)$ = 3.27 Oe observed for the aryl benzyloxy nitroxide radical are also consistent with those in the aforementioned studies.

Previous ESR work by Davis, Wilkes, Pugh, and Dorey[3] assigned the primary radicals observed in photodecomposition of energetic materials (TNT, DNT, TNB, and DNB) in various solvents to radical anions of the energetic material species. In light of our results for the TNB/toluene reactions and the experiments on nitrobenzene and TNB in THF, the radicals observed in Davis' study provide a more consistent picture with assignment as aryl alkyloxy nitroxide radicals. In our experiments with TNB in toluene, one would expect that a radical anion would not be stable in the nonpolar environment and would rapidly collapse into an aryl benzyloxy nitroxide radical even if the possibility of a contact ion pair is considered. This, however, does not dismiss the possibility of the reaction involved proceeding through a transition state where an electron transfer produces the radical anion/cation pair before the bond between the nitroxide oxygen and the solvent carbon is formed. If the radical ion were present in the reaction mixture, one would also expect that it would exhibit hyperfine splittings of about a_N = 2 Oe. This is consistent with known radical anion systems even if solvent effects are assumed to account for asymmetry of spin distribution.[10,13,36] Furthermore, the invariance of the nitrogen hyperfine splittings between toluene and THF as solvents discounts the radical anion interpretation. This invariance suggests that the species present is a neutral radical.

B. 3,5-Dinitrophenyl Benzyl Nitroxide Radicals. The secondary radicals observed in the photodecomposition after the solutions are heated to 290 K possess hyperfine splittings and signal intensity ratios consistent with previously observed aryl benzyl nitroxide species (lower traces of Figures 2, 4, 6, and 8).[14,20,22,23,30,33] The aryl benzyl nitroxide and aryl alkyl nitroxide radicals exhibit nitrogen hyperfine splittings in the range of 9–11 Oe, aryl hydrogen splittings in the range of 0.5–3 Oe, and magnetically equivalent β-hydrogen splittings in the vicinity of 4–6 Oe. The g value of 2.0061 ± 0.0003 for the radicals observed in the present study is in good agreement with those observed in the decomposition of related materials.[14,30,33-35]

The low-temperature ESR spectra of the aryl benzyl nitroxide radicals shown in the upper traces of Figures 2, 4, 6, and 8 possess magnetically inequivalent hyperfine splittings from the benzyl hydrogens. At low temperature, these splittings are a_H = 6.71 and 3.21 Oe, respectively. We are currently studying the temperature effects on the β hyperfine splitting in these systems. The results of this work will be reported in a future publication.[37] Briefly, these studies suggest the aryl benzyl nitroxide radicals exhibit a temperature dependence regarding the benzyl hydrogens where the magnetically equivalent hydrogens become inequivalent at temperatures below 230 K (refer to structures a and b for

SCHEME I

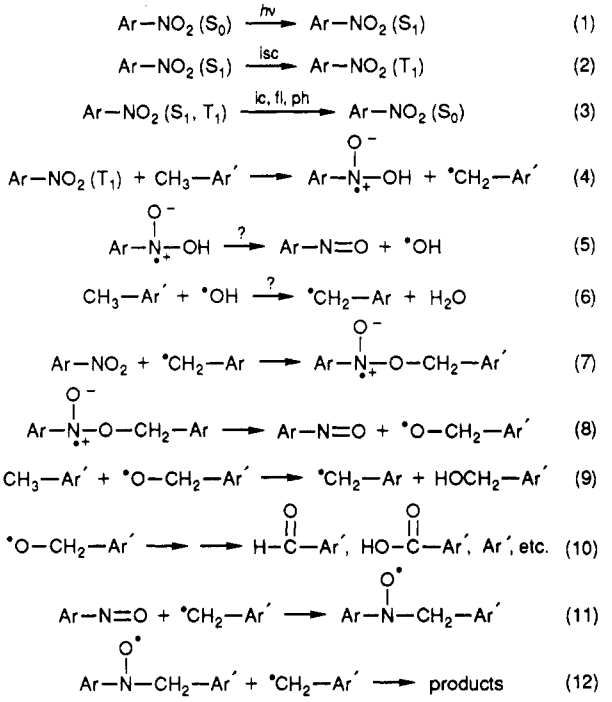

radicals II, IV, VI, and VIII in Table I). At these temperatures, mixtures of paramagnetic species are observed in the ESR spectra that can be attributed to aryl benzyl nitroxide species with equivalent benzyl hydrogens and aryl benzyl nitroxide species with inequivalent benzyl hydrogens. The relative populations of these two species in the ESR spectra varies markedly with temperature. At temperatures above 230 K, the species with magnetically equivalent hydrogens is dominant (lower traces in Figures 2, 4, 6, and 8). At temperatures below 230 K, the population of species with magnetically inequivalent hydrogens increases until about 195 K where it appears that it is the dominant species present (upper traces in Figures 2, 4, 6, and 8). The temperature dependence appears to be reversible in that samples can be temperature-cycled and the effect is reproducible. We are tentatively attributing this phenomenon to hindered rotation of the benzyl group attached to the nitroxide nitrogen. At higher temperatures, internal rotation about the C–N bond occurs, more or less, freely. The internal rotation may be complete or could be a large amplitude libratory motion. Thus, the benzyl hydrogens appear to be magnetically equivalent. At lower temperatures, the hydrogens become magnetically inequivalent since two conformations are expected that arise from barriers to internal rotation. The barriers may be identified as the points where the aromatic ring attached to the benzyl carbon eclipses the nitroxide oxygen or where it eclipses the aromatic ring attached to the nitroxide nitrogen. The potential surface for this motion has been calculated with MNDO/PM3[38,39] semiempirical methods as implemented in MOPAC version 5.0.[40] The results suggest that the aforementioned barriers to internal rotation are plausible causes of the anisotropic environment, resulting in the benzyl hydrogen magnetic inequivalence. A similar observation has been made when *N*-nitrosodimethylamine in toluene is photolyzed at low temperature.[34]

C. Mechanistic Scheme for the Photodecomposition. Experimental observation of aryl benzyloxy nitroxide and aryl benzyl nitroxide radicals in the photodecomposition of TNB in toluene suggests that the mechanism in Scheme I (where Ar = aryl group) could account for the formation of the species. Previous work[14,22,32] on nitroaromatic compounds suggests that hydrogen abstraction

(36) Gutch, C. J. W.; Waters, W. A.; Symons, M. R. C. *J. Chem. Soc. B* **1970**, *7*, 1261.
(37) Menapace, J. A.; Marlin, J. E.; Godec, G. E. Manuscript in preparation.
(38) Stewart, J. J. P. *J. Comput. Chem.* **1989**, *10*, 209.
(39) Stewart, J. J. P. *J. Comput. Chem.* **1989**, *10*, 221.
(40) Stewart, J. J. P. MOPAC 5.0: A General Molecular Orbital Package. *QCPE* **1989**, *No. 455*.

from the solvent by TNB can occur via an excited triplet state of TNB in the photodecomposition (reactions 1–4). The exact nature of the triplet state ($n-\pi^*$ or $\pi-\pi^*$) is not known; however, evidence of the latter state being the active species in the photodecomposition has been observed.[14,32] The hydrogen abstraction most likely occurs as shown in reaction 4 for which excited-state TNB reacts with the solvent yielding a benzyl radical and an aryl hydroxy nitroxide intermediate. Neither of these two radicals are observed in our experiments. This could be due to low steady-state concentrations resulting from reactions such as reactions 4 and 5. Experimental evidence of the aryl hydroxy nitroxide radical and similar species has been obtained in solutions of chloronitrobenzenes[22] and nitrosoalkanes.[33] The formation of the aryl benzyloxy nitroxide moiety can be assumed to occur by reaction 7 where the benzyl radical reacts with TNB. Similar observations for reactions of this type have been reported for nitroaromatic compounds in THF.[18-22] The paramagnetic intermediate subsequently decomposes to a nitrosobenzene moiety and a benzyloxy radical (reaction 8). The fate of the benzyloxy radical may involve quenching and oxidation reactions similar to those outlined in reactions 9 and 10. The corresponding alcohol, aldehyde, and acid products resulting from decomposition of TNB and TNT have been observed via HPLC analysis[41] and in thermal decomposition of molten TNT.[42] The formation of the aryl benzyl nitroxide species occurs via reaction 11 where a benzyl radical attacks the nitrosobenzene intermediate. This reaction has also been proposed in both photochemical and thermal decomposition studies.[2,4,14,20,22,30] Further reaction of the aryl benzyl nitroxide radical with the benzyl radical may involve continued reduction of the other nitro functionalities on TNB by reactions similar to reactions 1–11. Polymerization of TNT to form "explosive coke" is presumed to occur via a similar mechanism.[4]

V. Summary and Conclusions

ESR spectroscopy is used to probe the low-temperature photodecomposition of TNB in toluene. Solutions of TNB in toluene along with their deuteriated analogues are photolyzed at 200 K. Spectroscopic observables measured from the resulting ESR spectra such as hyperfine splittings, signal intensity ratios, and g values allow for the elucidation of the paramagnetic intermediates present in the photodecomposition event. Several conclusions are obtained regarding the details of the photodecomposition scheme and the characteristics of the radicals involved:

(1) The primary radicals observed during the low-temperature photodecomposition suggest, for the first time, that aryl benzyloxy nitroxide species are present as precursors to secondary radicals that can be attributed to aryl benzyl nitroxide radical intermediates. The radicals possess spectroscopic characteristics in agreement with adducts observed in the photodecomposition of similar nitroaromatic compounds in THF. Furthermore, the observation of the aryl benzyloxy nitroxide intermediates in toluene, a nonpolar solvent, suggests that previous assignment[3] of the species as radical anions is incorrect.

(2) The primary radicals appear to be relatively unstable compared to the secondary radicals. These radicals can only be observed in the low-temperature environment since their decomposition rate appears to be slow enough at 200 K to yield sufficient steady-state concentration for observation. Even at low temperatures, a significant amount of secondary radical is present. When compared to the primary radicals observed in the photodecomposition of TNB or nitrobenzene in THF, the corresponding radicals in the present study are not as stable. The primary radicals in the TNB/THF and nitrobenzene/THF studies do not appear to be contaminated with secondary radicals at room temperature. In these instances, significant amounts of the secondary radicals appear only after the much slower dark reaction takes place.

(3) The difference in stability between the aryl benzyloxy nitroxide and the aryl alkyl nitroxide radicals may involve the nature of the benzyl subunit compared to the corresponding subunit derived from THF. The former subunit may yield a less stable intermediate due to steric interactions with the aryl nitroxide subunit. Furthermore, the presence of the oxygen atom in the latter radical adduct allows for radical stabilization via oxygen lone pair interaction. Further studies on the photodecomposition of TNB in anisole are currently being conducted to explore these possibilities.

(4) The primary radicals decompose over time at 200 K or if the solutions are heated to 290 K in a dark reaction to yield secondary radicals. After the dark reaction, temperature cycling of the solutions between 200 and 290 K indicates that virtually all of the primary radical is consumed and that the primary radical may be construed as a precursor to the secondary radical.

(5) A temperature dependence of the benzyl hydrogens in the aryl benzyl nitroxide radical is observed that indicates that barriers to internal rotation exist for rotation about the C–N bond. The phenomenon is reversible and reproducible with a temperature change. At temperatures above 230 K, the benzyl hydrogens appear to be magnetically equivalent as evidenced by equal magnitudes of their corresponding hyperfine splittings. Below 230 K, the benzyl hydrogens become magnetically inequivalent, which most likely occurs from the "freezing out" of two possible conformers that arise from barriers involving the eclipsing of the nitroxyl oxygen or from the aryl substituent with the phenyl ring adjacent to the benzyl carbon.

Acknowledgment. The Air Force Office of Scientific Research, Directorate of Chemical and Atmospheric Sciences, is gratefully acknowledged for funding this study under Project 2303-F3-05. S. W. Lander, S. A. Shackelford, and J. J. P. Stewart provided helpful scientific discussion and manuscript review. C. R. Edmundson, Jr., assisted in the development of the ESR spectrum graphics software used in the figure preparation.

Registry No. I, 123933-83-5; II, 123933-84-6; III, 123933-85-7; IV, 123962-96-9; V, 123933-86-8; VI, 123933-87-9; VII, 123933-88-0; VIII, 123933-89-1; IX, 123933-90-4; X, 123933-91-5; XI, 22047-11-6; XII, 123933-92-6; TNB, 99-35-4; TNB-d_3, 14702-07-9; toluene, 108-88-3; toluene-d_8, 2037-26-5.

(41) Menapace, J. A. Unpublished results. Menapace, J. A.; Swanson, J. T. Unpublished results.

(42) Dacons, J. C.; Adolph, H. G.; Kamlet, M. J. *J. Phys. Chem.* **1970**, *74*, 3035.